

# Development of a Calibration Satellite for a CMB Telescope Flying in Formation about L2 Libration Point

Juan Bermejo-Ballesteros<sup>1†</sup>, Sergio García-González<sup>1</sup>, Javier Cubas<sup>1</sup>,  
Francisco Javier Casas Reinares<sup>2</sup>, Enrique Martínez González<sup>2</sup>

<sup>1</sup>*Instituto Universitario de Microgravedad Ignacio da Riva, Universidad Politécnica de Madrid  
Plaza Cardenal Cisneros, 3, 28040 Madrid, Spain*

<sup>2</sup>*Instituto de Física de Cantabria (CSIC-UC)*

juan.bermejo@upm.es

†Corresponding author

## Abstract

The new generation of cosmic microwave background (CMB) telescopes have reached unprecedented levels of sensitivity. These telescopes measure several cosmological parameters with different levels of accuracy. In particular, considerable effort has been made to measure the B-mode polarization, which is related to the inflationary process of the universe. The power spectrum of this signal is about four orders of magnitude fainter than the CMB temperature power spectrum. Due to the signal weakness, the instruments must be subjected to calibration processes before and after launching. Additionally, data from the same sky area is gathered repeatedly to mitigate during data analysis the systematic errors induced by instruments. Celestial sources are often used as an external reference for calibration after launch, but these sources are not perfectly characterized. In this paper we study the concept of using a calibration satellite (CalSat) flying in formation with a CMB telescope in an orbit located at the second Lagrange point (L2). The CalSat is conceived as a micro satellite (10-100 kg) and serves as a perfectly known source of a reference signal to reduce the polarization angle measurement uncertainty. According to the scanning law followed by the telescope, the influence of the relative position between the spacecrafts in the calibration process is studied. The relative motion of the spacecrafts is considered with a simplified dynamic model. Based on the mission requirements, the different subsystems are sized and a preliminary design to evaluate the feasibility is obtained. The design has been carried out under the principle of reducing at minimum the impact on the telescope architecture. It would require to be launched along with the telescope to reach L2 at the same time and being able to communicate with the telescope. This new calibration element could have a huge impact on the performance of this kind of missions, providing a significant improvement in the measurements accuracy without requiring new and costly technological developments.

## 1. Introduction

The cosmic microwave background (CMB) is a faint electromagnetic radiation originating from all directions in space. The CMB spectrum is the same as that of a black body at a temperature of approximately 2.7 K. However, there are anisotropies in both the CMB intensity and polarization that can be measured to investigate early universe characteristics. In particular, the polarization of the CMB is measured and decomposed in two types of polarization, B-mode and E-mode. The B-mode polarization has raised attention in recent years, with several planned space missions focused in measuring it, as it is related to the inflation of the universe. In order to measure these faint signals, CMB telescopes have become increasingly sensitive. In this context, it is mandatory to address the mitigation of instrument-induced systematic errors, which is done during data analysis. One of the systematic errors to be reduced is the instrument-induced polarization (IPR), which converts the brighter E-modes into B-modes.

In Johnson et al<sup>1</sup> is presented a space mission concept to reduce this error by the observation of a linearly polarized source with well-characterized polarization properties. This signal is emitted by a CubeSat (named CalSat) orbiting Earth that would be observed by Earth-based CMB telescopes. In this paper, it is studied the concept of calibration satellite for CMB telescopes on board satellites located in the second Lagrangian Point (L<sub>2</sub>). This location is of particular interest in all kind of space observation satellites as it allows continuous sky observation (although it requires half

## CALIBRATION SATELLITE FOR CMB TELESCOPE

a year to observe the whole sky) and a thermally stable environment, ideal for cryogenic systems. In particular, two CMB missions located at  $L_2$  have already ended (WMAP and Planck) and one (LiteBIRD) has been already selected by JAXA to be launched in 2027.

The CalSat proposed in this paper is a micro-satellite (10-100 kg) that would flight in formation with a CMB telescope in the vicinity of the second Lagrange point of the Sun-Earth system. Based on a set of top-level requirements, the mission is analyzed in several aspects, relative motion, calibration process and attitude determination error propagation. The results of these analysis lead to more specific requirements that are used then to size and preliminary design the main subsystems of the calibration satellite. Finally, the feasibility of the mission concept is evaluated. The mission has been studied under the principle of reducing at minimum the impact on the telescope architecture.

## 2. Mission

### 2.1 Overview

For the mission study, the CMB telescope is assumed to have a Lissajous orbit around  $L_2$  similar to that of Planck and WMAP. Both satellites, CalSat and CMB telescope would be put in orbit simultaneously by the same launcher and CalSat would reach  $L_2$  by its own means to minimize impact in the telescope architecture. Once in  $L_2$ , the CMB telescope carries out its scientific mission routinely while the CalSat stands by in the surroundings, out of sight from the telescope instrument. Periodically, the CMB telescope requires calibration and the CalSat relocates itself so it can be adequately observed by the telescope instrument. Once the calibration has taken place, the CalSat gets back to its stand-by position. The mission is expected to last three years.

The CalSat mission can be divided in two phases, transfer and operation. In this paper, we focus in the operation phase, although the transfer phase is considered in terms of required  $\Delta v$ . In turn, operation phase is divided in two modes, stand-by mode and calibration mode. CalSat will spend most of the mission in stand-by mode, maintaining a minimum safe distance. Maximum distance is not as important, providing that CalSat can get close again without requiring major maneuvers. In comparison, during calibration mode CalSat will keep a fixed relative position within a margin. This position will place the CalSat in the far field of the telescope.

As outlined by Johnson et al<sup>1</sup>, during the calibration process the CalSat payload would emit several signals in different frequency bands. These linearly polarized signals would serve as reference for characterize the IPR effect in the polarimeters of the CMB telescope. The calibration provides an accurate relationship between the coordinate system of each polarimeter in the instrument frame and the coordinate system on the sky. The threshold for the error in the polarization angle has been taken from the estimation for the future mission LiteBIRD<sup>2</sup>, where it is established in 3 arcmin.

Although called calibration process, the CalSat crossing of the telescope field of view (FOV) does not produce an immediate calibration. The error mitigation is done during data analysis back in Earth, after downloading telescope observation data. Thus, the attitude and position of CalSat during the calibration process must be sent to Earth. Also, there must be an indication of when the calibration process will start to minimize the duration of the task.

From the description of the mission, a set of top-level requirements are established. These requirements are used for studying three aspects of the mission in more detail: mission analysis, visibility study of the CalSat according to its position and attitude determination error propagation. The results of these analysis are then used to derive more specific requirements that drive the preliminary sizing and design of the CalSat subsystems. The top-level requirements are listed below:

- Lissajous orbit around  $L_2$
- To reach  $L_2$  autonomously
- Mission duration of 3 years
- To maintain minimum distance of 240 m with CMB telescope
- To maintain calibration distance of 270 m within an error of 0.05%

- To measure line of sight direction between CalSat and telescope within 0.1% error
- Angular uncertainty of the signal received by CMB telescope below 3 arcmin
- Minimum communication with CMB telescope to set calibration process start
- To perform at least one calibration per month
- To be able to send data to Earth
- To accommodate and operate the required payload

## 2.2 Mission Analysis

The primary objectives of this mission analysis are two: first, to evaluate how significant is the drift between satellites in short periods of time (compared to mission duration) and second, to obtain an estimation of the  $\Delta v$  required for the mission. The drift between the satellites is studied using simulations to assess its impact during the calibration process and as for the  $\Delta v$  estimation, available literature is reviewed to obtain projections for four activities: transference to  $L_2$ , orbit maintenance during stand-by mode, relocation maneuvers from stand-by position to calibrating position and formation maneuvers to maintain the formation during the calibration process.

The formation is studied under the chief-deputy configuration, where the CMB telescope (chief) is assumed to follow a 'natural' Lissajous orbit around the Sun-Earth second Lagrange point ( $L_2$ ) and the calibration satellite (deputy) performs the required manoeuvres to maintain the desired relative position (distance and orientation) within a margin. The dynamical environment of this location is adequate for a flight formation as it requires low orbit maintenance and the low accelerations and velocities potentially enable high precision formations.

The relative motion of the spacecrafts is studied directly through the simplified dynamical model of the Circular Restricted Three-Body Problem (CRTBP) applied to the Sun-Earth system. This model describes the dynamics of a body whose mass is negligible compared with two celestial bodies (primaries). The main assumptions of this model are that the primaries are considered to have circular orbits and perturbations are not taken into account. The study of this problem is simplified by using a synodic reference frame and normalizing the equations of motion<sup>3</sup>. As shown in Figure 1, the reference system is centered in the Sun-Earth barycenter, with the X-axis passing through the Sun and the Earth and oriented to the latter, and the XY-plane lying in the ecliptic plane.

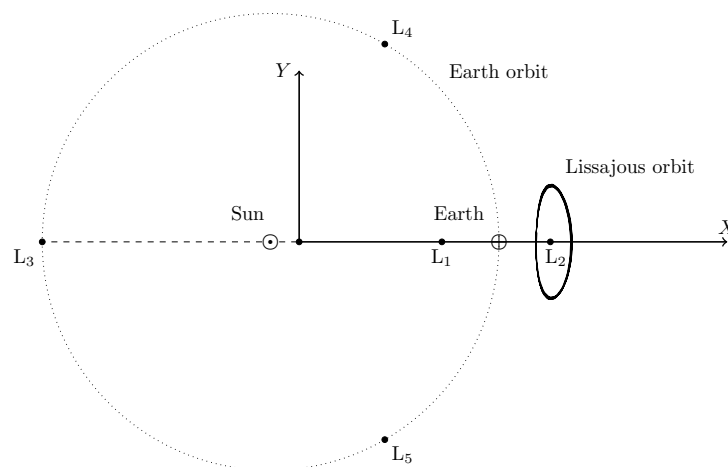


Figure 1: Synodic Reference Frame and Lissajous orbit view from Z direction. Not to scale.

The equations of motion after transforming them to the rotating, normalized reference frame become:

## CALIBRATION SATELLITE FOR CMB TELESCOPE

$$\begin{aligned}
\ddot{x} - 2\dot{y} &= \frac{\partial U}{\partial x} \\
\ddot{y} + 2\dot{x} &= \frac{\partial U}{\partial y} \\
\ddot{z} &= \frac{\partial U}{\partial z}
\end{aligned} \tag{1}$$

where  $U$  is a pseudo-potential function defined as:

$$U = \frac{1}{2}(x^2 + y^2) + \frac{1-\mu}{r_1} + \frac{\mu}{r_2} \tag{2}$$

and  $\mu = m_2/m_1$ , the mass ratio between the primaries which must not be mistaken with standard gravitational parameter.  $r_1$  and  $r_2$  are the distances from the primaries to the third body. These equations present 5 equilibrium points, the so called Lagrange libration points, whose location is shown in Figure 1. The collinear points ( $L_1$ ,  $L_2$  and  $L_3$ ) are unstable and if not maintained, any orbit around them will end up escaping from the libration point region and entering a heliocentric orbit. Conversely, the equilateral points ( $L_4$  and  $L_5$ ) are stable. For this mission analysis, it has been selected a Lissajous orbit of amplitudes  $A_y = 350000$  km and  $A_z = 300000$  km, similar to Planck. The nominal path, followed by the telescope, has been generated using the method described by Howell<sup>4</sup>.

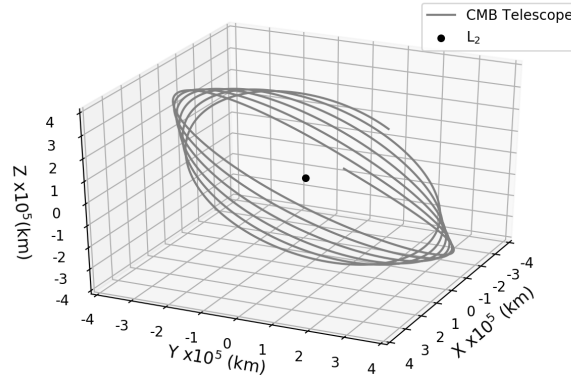


Figure 2: Nominal path of the telescope. It is a Lissajous orbit around  $L_2$  of the Sun-Earth system with amplitudes  $A_y = 350000$  km and  $A_z = 300000$  km.

The simulation of the relative motion has been carried out integrating (1) directly for the deputy, with the same initial conditions as the chief but with a given initial displacement of 270 m in different directions that conform a semi-sphere centered in the chief and with its main axis parallel to +X. The movement is propagated for three different time periods: 60 seconds, 1 hour and 1 day. Then, the displacement from initial relative position and the angular displacement of the line of sight are evaluated. In Figures 3 and 4 are shown the results for 1 hour of propagation. This analysis is based on the work of Héritier et al<sup>5</sup>. In these pictures, points indicate the position of the deputy regarding the chief in the initial instant and the color of the point represent the magnitude of the displacement. The results for 60 seconds and 1 day are similar to those of 1 hour, with nearly the same distribution of low and high displacements but with different maximum values. In Table 1, the maximum drifts in the three different periods of time are shown.

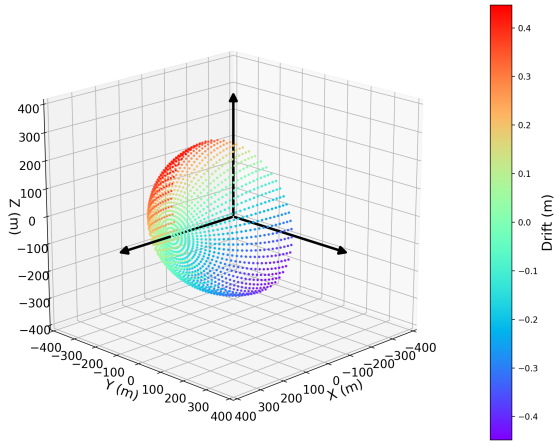


Figure 3: Semi-sphere of positions displaying the drift experienced by the deputy after 1 hour.

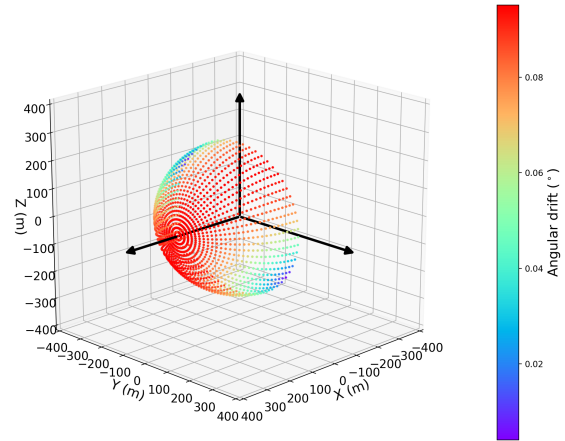


Figure 4: Semi-sphere of positions displaying the angular drift experienced by the deputy after 1 hour.

Table 1: Maximum values of drift and angular drift for different time periods.

	$\ \Delta r\ _{max}$ (m)	$\ \Delta\theta\ _{max}$
60 s	1.5E-2	12.5''
1 h	0.4	6'
1 day	10	2.25°

As the study of transference from Earth and orbit maintenance are not the aim of this paper, estimations of  $\Delta v$  from Planck mission analysis<sup>6</sup> are taken as reference value. The calibration maneuvers to entering and exiting the instrument FOV are studied through a simplified model, with the synodic reference frame centered in the chief and under the assumption that, for short periods of time, the reference system can be considered inertial. In Table 2 are summarized the results of this study.

Table 2:  $\Delta v$  budget for three years mission.

Activity	$\Delta v_T$ (m/s)
Transfer from parking orbit to L <sub>2</sub>	293
Orbit maintenance	3
Relocation maneuvers	3
Formation maneuvers	1
Total	300

The results of the mission analysis indicate that the drift for short periods of time is negligible. Thus, the changes due to the orbital movement can be ignored for short periods of time (several hours). This assumption will be used in the analysis of following sections. It should be noted that, for this simulations, the deputy remains uncontrolled, as the deputy has the same initial velocity as the chief and no  $\Delta v$  is applied in any moment. The drift could be potentially reduced up to 1 cm for periods of several days according to Pernicka et al<sup>7</sup>. However, such precision can entail maneuvers with a  $\Delta v$  prohibitively low. In the CalSat case, it would only be necessary to maintain the drift below 13.5 cm (0.05% of 270 m) during a period of hours, thus allowing to perform not so small maneuvers.

Regarding the  $\Delta v$  budget, the transference maneuver to L<sub>2</sub> demands the greater allocation whereas the orbit maintenance maneuvers (applied during stand-by mode) represents an average of 1 m/s per year of mission. The same applies to the relocation maneuvers. For formation maneuvers, 1 m/s has been allocated although the expected consumption is lower.

## CALIBRATION SATELLITE FOR CMB TELESCOPE

## 2.3 Visibility analysis

As previously said, the purpose of CalSat is to serve as a reference source providing a known linearly polarized signal. In order to calibrate the telescope instrument, the CalSat must be inside its field of view, which will not always be true due to the attitude movement of the telescope. The frequency and duration of these events, which will be called ‘accesses’, are determined by the relative position between the satellites and the scanning law of the telescope. Studying how these two parameters evolve as the relative position changes will allow to define an optimal position for CalSat in order to be seen from the telescope and to establish constraints in the design of the satellite. Furthermore, this study will provide data about how the signal is received by the telescope instrument.

The telescope attitude changes according to its scan strategy, which is chosen primarily to sample all the sky in a certain period of time and to do it recurrently in order to mitigate systematic errors. The model implemented is based on Wallis et al<sup>8</sup> but in this case only four parameters have been used ( $T_{spin}$ ,  $T_{prec}$ ,  $\alpha$  and  $\beta$ ). The satellite spins around its main axis with a time period of  $T_{spin}$ . The line of sight of the instrument forms an angle ( $\beta$ ) with the spin axis. Simultaneously, the satellite spin axis precesses around an axis that is parallel to the line passing through the Sun and the Earth. The angle between these axes is called  $\alpha$  and the period time  $T_{prec}$ . The region of observation lies in the anti-Sun direction. An scheme of the scan law is shown in Figure 5.

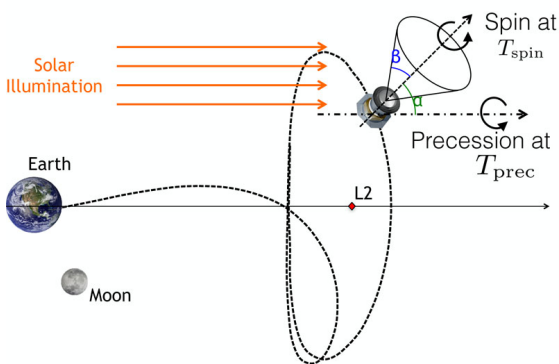


Figure 5: Scan law scheme. Extracted from Wallis et al<sup>8</sup>.

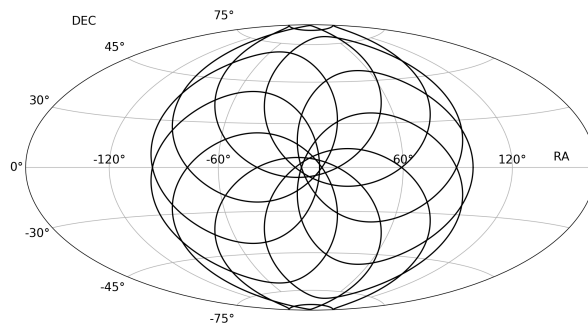


Figure 6: Hammer projection of the scan pattern over the celestial sphere. RA stands for right ascension and DEC for declination.

As the aim of this analysis is not to study the adequacy of the scan strategy but rather to investigate the influence of the CalSat relative position to the telescope, only one scanning law has been considered ( $T_{spin} = 10$  min,  $T_{prec} = 90$  min,  $\alpha = 50^\circ$  and  $\beta = 45^\circ$ ). These parameters build a pattern of observation over the celestial sphere, this is, the trace of the telescope instrument, of which a projection is depicted in Figure 6. As both movements are periodic, a higher period of the combined movement will produce a finer pattern.

A series of simulations with the CalSat located in different positions have been carried out in order to obtain accesses distribution and duration. An access occurs when the CalSat enters the field of view of the telescope instrument, which is defined by the instrument main axis and an aperture of  $15^\circ$ . The relative positions considered conform a semi-sphere around the CMB telescope and oriented to +X, similar to the one shown in Figures 3 and 4. The time simulated is equal to the period of one precession revolution, 1.5 h.

The results of this first simulation are showed in the Figures 7 and 8, where total access time ( $T_{total}$ ) and mean access time ( $T_{mean}$ ) are plotted for all the locations considered. For the representation of the results, a Hammer projection of the whole celestial sphere is been used.  $T_{mean}$  is roughly 30 s in most cases and  $T_{total}$  depends on the total number of accesses.

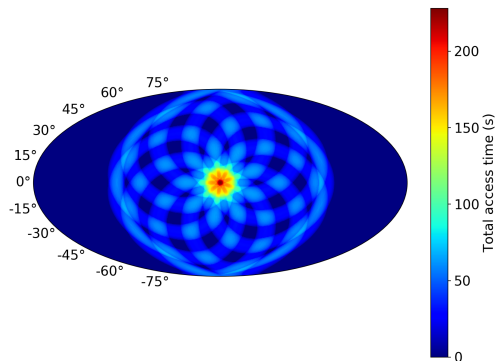


Figure 7: Total time of access after 90 minutes.

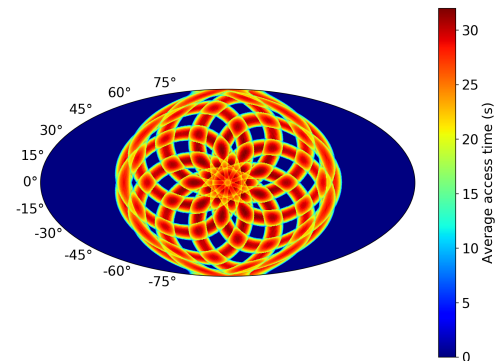


Figure 8: Average time per access after 90 min.

In the Figure 9, the distribution of the accesses along time and the duration of each one of them is shown. These results correspond to a reduced set of locations, with a fixed declination of  $0^\circ$  and an interval of right ascension of  $0^\circ$  to  $30^\circ$ . Nevertheless, the figure shows the trend in the number of events and duration, this pattern repeats over time. In order to have a higher number of accesses, the CalSat should be located close to +X axis. If CalSat has a right ascension higher than roughly  $15^\circ$ , there will be only one access and the waiting time between accesses would be equal to one precession period, 1.5 h. It should be noted that even in the best case, the waiting time is at least of 10 min.

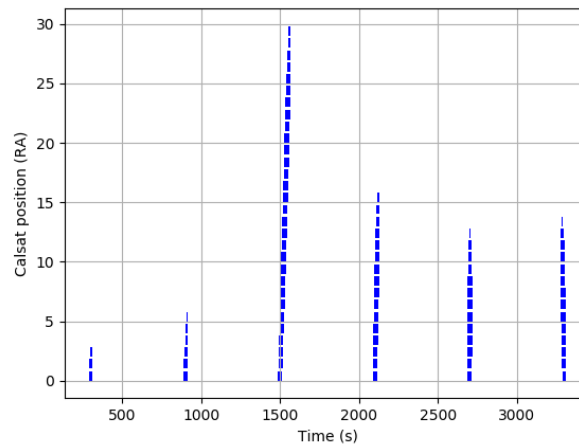


Figure 9: Distribution of accesses along time and their duration according to the CalSat position.

The polarimeter detectors of the main instrument of a CMB telescope are made of bolometers, which measure the power of incident electromagnetic radiation. The number of bolometers of such an instrument is usually around several thousands. The more bolometers can be calibrated, the better measurements accuracy. For this reason, it is interesting to quantify how many of these bolometers would detect the reference signal emitted by the CalSat as a function of the calibration satellite position, relative to the chief. The density of the viewed sensors,  $\rho_{sensors}$ , is defined as the ratio between the viewed bolometers and the total number of bolometers, expressed as a percentage. As in previous sections, simulations for different CalSat positions conforming a semi-sphere and for a time period of 1.5 hours have been carried out.

In this analysis, the calibration signal projection on the main satellite has been considered to be a punctual source while the main telescope instrument has been modelled as an array of 2124 quadrangular elements which represent the bolometers.

## CALIBRATION SATELLITE FOR CMB TELESCOPE

The trace of the CalSat on the main satellite instrument is shown in Figure 10, during 90 minutes for an specific position of the calibration satellite. Each different CalSat trace (each curve that is projected onto the instrument plane shown in Figure 10) belongs to a different access. This same result has been obtained for all the different position of the CalSat and gathered in Figure 11.

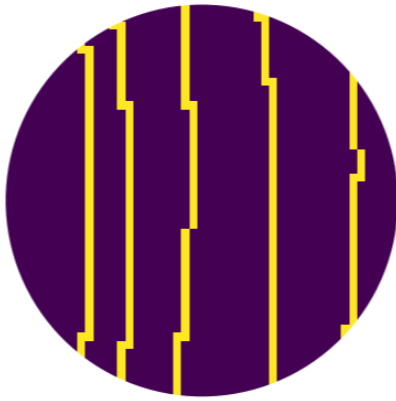


Figure 10: Example of CalSat trace on the main telescope when the calibration satellite is near the maximum  $\rho_{sensors}$  area (declination equal to  $3^\circ$  and a right ascension of  $8^\circ$ ).

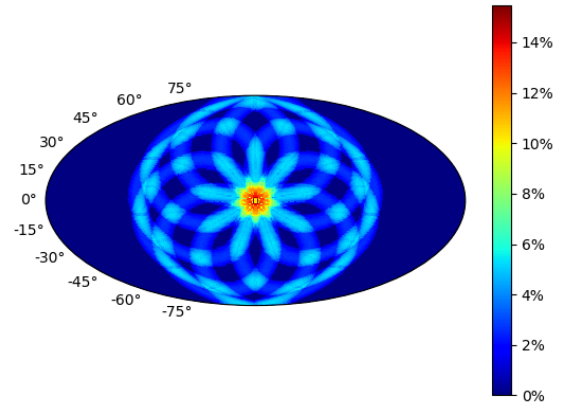


Figure 11: Hammer projection of the viewed bolometer density ( $\rho_{sensors}$ ) for all possible positions of the calibration satellite throughout 90 minutes.

The more separated the different traces are, the greater the sensor density will be. In the example shown in Figure 10 the different passes are spread through the whole instrument and this situation represents a maximum in the viewed sensor density. As proved in Figure 11, the ideal situation to calibrate as many bolometers as possible would be to place the calibration satellite on the surrounding of the chief precession axis (anti-Sun direction) but not exactly there.

## 2.4 Attitude determination analysis

The objective of the calibration is to reduce the absolute polarization angle uncertainty of the telescope instrument. To do this, the calibrating satellite emits a reference signal that will be detected by the main satellite instrument. By definition, the polarization of this reference signal is measured in the plane perpendicular to the line connecting the CalSat and the telescope. The difference between the polarization angle of emission and the polarization angle measured by the instrument will be used to calibrate the reference system of the bolometers that compose the instrument. Both the emission angle and the measured angle have an associated uncertainty due to the limited precision of the Attitude Determination and Control System (ADCS) of each satellite. Thus, the difference of both angles will have its own uncertainty result of the combination of the two ADCS errors. In this section, it has been studied how accurately would be necessary to know the CalSat attitude in order to achieve the required angular uncertainty threshold established in the requirements.

Star trackers are presented as the only device capable of determining the attitude of the calibration satellite with enough accuracy for this mission, but even them are far from perfect. Angular errors around each axis of the star tracker define the misalignment between the real body frame attitude ( $BF^r$ ) and the measured one ( $BF^m$ ). When such angular errors are small enough to neglect second order terms, the transformation matrix between  $BF^m$  and  $BF^r$  can be expressed as<sup>9</sup>:

$$C^{BF^m-BF^r} = I + [\Delta\theta]_X, \quad (3)$$

where  $\Delta\theta = [\theta_x, \theta_y, \theta_z]$  is a vector composed of the misalignment angles around each body frame axis, the operator  $X$  refers to the skew matrix and  $I$  refers to the identity matrix. It is equivalent to three rotations around each specific axis,

regardless of the order and neglecting second order terms:

$$[\Delta\theta]_X = \begin{pmatrix} 0 & \theta_Z & -\theta_Y \\ -\theta_Z & 0 & \theta_X \\ \theta_Y & -\theta_X & 0 \end{pmatrix}. \quad (4)$$

Usually, the angular error around the star tracker boresight axis is larger than around the other axes (approximately three times larger). For that reason, the misalignment angles of the calibration satellite star tracker will be defined as

$$\Delta\theta = [3\theta_{ST}, \theta_{ST}, \theta_{ST}]. \quad (5)$$

Given a known direction in the body frame of a satellite, the matrix  $C^{BF^m-BF^r}$  allows to obtain a ‘measured’ direction that includes the error of the attitude determination. In this study, the polarization of the signal is modeled as the angle that forms a unit vector with the X-axis of a reference system whose XY-plane is perpendicular to the line between chief and deputy. The direction of the X-axis is not significant as it is differences in angles what is being calculated. Assuming that the chief attitude determination system adds a conservative uncertainty to the process, given by

$$\Delta\theta = [60'', 20'', 20''] \quad (6)$$

the maximum angular error on the bolometer plane is shown, as a function of  $\theta_{ST}$ , in Figure 12. The angular error  $\Delta\beta_{max}$ , shown in Figure 13, is defined as the maximum angle between the nominal polarization vector of the reference signal projected on the bolometers plane (without considering attitude errors), labeled as  $\beta_0$ , and the actual one taking into account the star trackers uncertainties, labeled as  $\beta$ . This reference signal polarization is used to calibrate the bolometer reference frame. Therefore, it is a crucial element for obtaining accurate bolometer measurements.

As shown in Figure 12,  $\Delta\beta_{max}$  is a linear function of the  $\theta_{ST}$  variable. However, this only happens because the range of  $\theta_{ST}$  explored is small. For larger values of  $\theta_{ST}$ , the linear behaviour disappears. The angular error  $\Delta\beta_{max}$  has been determined considering the actual scanning law of the telescope described in Section 2.3 with the CalSat emitting the reference signal (although we are interested in its polarization) in the direction of the chief during 90 minutes. The uncertainties of the calibration satellite and the chief in its attitude determination, given by (5) and (6), are responsible for the differences between the nominal polarization signal and the received one on the instrument plane, where the bolometers lie.

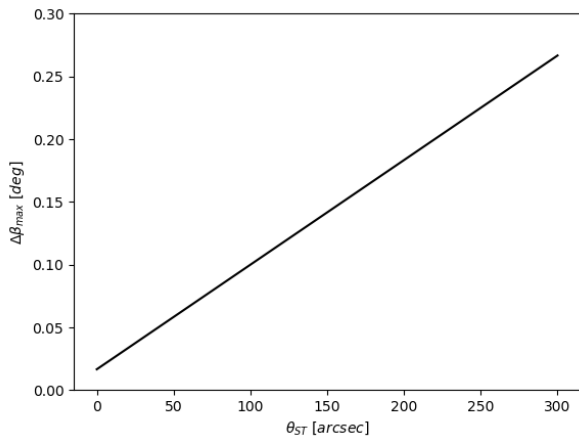


Figure 12: Maximum uncertainty in the bolometer reference frame as a function of the CalSat star tracker accuracy.

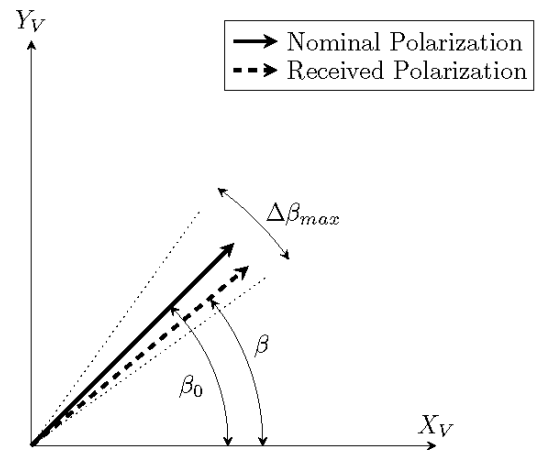


Figure 13: Bolometer reference frame and projected signal representation.

Given that the maximum angular error on the bolometer plane must be lower than 3 arcmin, that means that  $\Delta\beta_{max} = \max(|\beta - \beta_0|) < 3 \text{ arcmin}$ . As shown in Figure 12, the angular error of the calibration satellite star tracker must be lower

## CALIBRATION SATELLITE FOR CMB TELESCOPE

than 40 arcsec, which is achievable for most star trackers under the CalSat conditions.

## 2.5 Requirements

From the analysis made, the top-level requirements and further information about the payload and the CMB instruments, a set of requirements for the different subsystems are derived and listed below.

- **Mission**
  - Angular separation with +X axis < 12°
  - LOS measurement angular error < 0.1%
  - Calibration distance measurement error < 0.5%
- **ADCS**
  - Attitude determination error < 40 arcsec
  - Pointing error < 1°
- **Propulsion**
  - $\Delta v_T = 300$  m/s
  - $\Delta v_{min} = 10^{-5}$  m/s
- **Communications**
  - Reception of calibration start signal
  - Earth communications
- **Power**
  - Payload consumption of 28 W (duty cycle 3.5%)

## 3. Preliminary design

In this section, a preliminary design of CalSat based on the requirements is outlined. Main subsystem are briefly described and the main parameters that characterize them are provided.

### System

The CalSat is conceived as a micro-satellite with a maximum mass of 100 kg. Taking into account the  $\Delta v$  required for maneuvers and the specifications of the propulsion subsystem, the ratio between propellant mass and total mass is of roughly 13%. In order to determine the direction of the line of sight (LOS) with the telescope and measure the separating distance, RF-based relative navigation technology is considered as a adequate option<sup>10</sup>. This would require that some hardware (RF patch antennas) is installed in the CMB telescope but the power demanded would be low (roughly 1 W).

### Payload

The main payload is a set or radio frequency horns antennas with an estimated power consumption of 50 W while they operate. As most of the time the CalSat is not seen by the instrument, the duty cycle is low, which leads to an average consumption of 2 W. Nevertheless, the power subsystem shall be able to provide a peak of 50 W to the payload when demanded.

### Propulsion

The propulsion subsystem is required for orbital maneuvering and attitude control. In this mission, two types of orbital maneuvers are considered: high impulse and low impulse maneuvers. The former are required for the first stage of the mission, during the injection in the Lissajous orbit around L<sub>2</sub>. The low impulse maneuvers encompass the orbit

maintenance and the maneuvers performed before and after the calibration to relocate the deputy.

Based on the requirements of Section 2.5 and in the information of propulsion for micro-satellites gathered by Scharfe<sup>11</sup> it is proposed a monopropellant propulsion subsystem fueled with Hydrazine. In case that low impulses were required for small formation maneuvers, MEMS thrusters fueled with H<sub>2</sub>O<sub>2</sub> would provide<sup>12</sup> impulse bits of 1  $\mu$ N.

### ADCS

The CalSat has to be stabilized in all three axes. Due to the distance to the Earth, ADCS instruments that rely in Earth's proximity as horizon sensors or magnetometers are not available for its use in L<sub>2</sub>. Therefore, it is necessary to employ sun sensors and star trackers to determine the attitude and reaction wheels for its control.

The star trackers accuracy is enough to comply with the requirements for ADCS subsystem from Section 2.5, however, sun sensors are also included to point solar panels towards the Sun without using star trackers, whose power consumption is higher. The reaction wheels will allow the CalSat to point in the right direction during maneuvers, calibration and communications.

### Communications

The distance between L<sub>2</sub> and Earth (1.5 millions of km) makes it more difficult to communicate with ground stations compared to LEO orbits as pointing requirements are stricter and the signal strength must overcome a much larger distance. Seeking minimum modifications on telescope architecture, direct communication with Earth is considered for the subsystem design. Thus, a High Gain Antenna will be required, using X-Band as Planck and Herschel missions.

Nevertheless, it is necessary at least a minimal communication capability between the satellites, even though if it is a one-way signal from the telescope to the CalSat. This signal is required for setting the start of the calibration. The same system used for relative positioning can be easily adapted for such purpose.

### Power

The solar array area is estimated based on the average power that is necessary to generate taking into account the degradation of the solar cells and the efficiency of the system. The power consumption of the whole satellite is estimate to be about 80 W although, as not all the subsystem will be active at the same time, the average consumption would be 45 W (End of Life/EOL). Thus, the average power to generate at the beginning of the mission (Beginning of Life/BOL) is 60 W. The solar cells considered are triple junction.

Table 3: Overall system features.

Subsystem	Parameter	Value
System	Total mass	100 kg
	Propellant mass ratio	13%
Payload	Mass	1.2 kg
	Power	50 W
	Duty cycle	3.5%
Propulsion	Thrust	1 mN
	$I_{sp}$	215 s
	Propellant	Hydrazine
ADCS	Star Trackers accuracy	40 arcsec
	Sun sensors accuracy	3 arcmin
Communications	Band	X
	Antenna	Fixed High Gain Antenna
Power	Average power generated (BOL)	60 W
	Solar array area	0.3 m <sup>2</sup>

## 4. Conclusions

The possibility of employing the CalSat concept to calibrate CMB telescopes in the L2 libration point has been analyzed in the present document and the main conclusion drawn is that it is feasible. The CalSat can offer a unique source of calibration and opens the possibility of extend the concept for mitigation of other systematic errors or even calibrate other telescopes in the same region.

Several reasons lead to establish the region near the chief precession axis (but not exactly there) as the optimum zone to place the calibration satellite. There are more viewed sensors within this particular zone. The calibration signal projection in the main instrument is more spread in that case thus illuminating more bolometers. Additionally, this region presents the lower values of drift, which could prevent the need of formation maneuvers. Lastly, although being separated from the chief precession axis suppresses some of the potential accesses, it still presents up to 5 accesses, all consecutive, and with the same average duration.

In this study, a particular scanning law has been analyzed, defined by the four parameters described in Section 2.3 ( $T_{spin} = 10$  min,  $T_{prec} = 90$  min,  $\alpha = 50^\circ$  and  $\beta = 45^\circ$ ). As the  $T_{prec}/T_{spin}$  ratio is an integer, the CalSat trace will be repeated after precession period. It is possible to find different ratios in such a way that the repetition period of the trace will increase significantly. This leads to a finer pattern, which would modify some of the results presented here and could benefit the performance of the CalSat. This is not necessarily a drawback as it just represents a different scanning law of the telescope. In future analyses, other scanning laws (represented by different values of the four previous parameters) will be considered.

An important fact must be highlighted regarding the bolometers frame uncertainty requirement and the calibration satellite utility. The purpose of the CalSat is to offer a calibration source for telescopes around L<sub>2</sub> libration point. Both the main telescope and the calibration satellite have devices capable of determining their attitude with high accuracy. These devices are usually star trackers and, although they are really accurate, they are not perfect and uncertainties are always present in the attitude determination. Some analyses<sup>2</sup> establish a requirement in the maximum polarization angle error (directly related to the bolometer frame calibration) very similar to the telescope attitude uncertainty but they do not consider additional errors relative to the calibration process. In the CalSat case, these additional errors are the star tracker errors in the attitude determination of this satellite. For that reason, the polarization angle will be larger than the telescope attitude determination uncertainty.

In this study, we have consider the calibration satellite as a micro-satellite with a maximum mass of 100 kg mainly because it has been conceived to reach the L2 libration point by itself. However, the concept of CalSat can be easily extended to a CubeSat if two conditions are enforced: it would have to be deployed by the main telescope to avoid the expensive transference maneuver and it must meet the requirements stated in Section 3. Further studies will consider this option and its feasibility.

The viewed sensor density analysis shown in Section 2.3 has allowed us to draw conclusions about the best CalSat position based on how many bolometers are ‘illuminated’ by the reference signal. However, we have not considered here the crossing direction of that reference signal with respect to the bolometer frame. Different crossing directions imply different polarization angles (in the same bolometer) during different accesses and a broad variety of polarization angles has a positive effect on the bolometer frame calibration. For that reason, in future analyses, a direction analysis similar to the one shown in Figure 11 will be carried out.

## 5. Acknowledgments

The authors would like to thank Spanish Ministry for Economy and Competitiveness (currently Ministry of Science, innovation and Universities) for the financial support provided under the projects with references ESP2017-92135-EXP all co-financed with EU FEDER funds.

## References

- [1] Bradley R Johnson, Clement J Vourch, Timothy D Drysdale, Andrew Kalman, Steve Fujikawa, Brian Keating, and Jon Kaufman. A cubesat for calibrating ground-based and sub-orbital millimeter-wave polarimeters (calsat). *Journal of Astronomical Instrumentation*, 4(03n04):1550007, 2015.

- [2] Yutaro Sekimoto, Peter Ade, Kam Arnold, Jonathan Aumont, Jason Austermann, Carlo Baccigalupi, Anthony Banday, Ranajoy Banerji, Soumen Basak, Shawn Beckman, et al. Concept design of the litebird satellite for cmb b-mode polarization (conference presentation). In *Space Telescopes and Instrumentation 2018: Optical, Infrared, and Millimeter Wave*, volume 10698, page 106981Y. International Society for Optics and Photonics, 2018.
- [3] Victor Szebehely. Theory of orbits: the restricted problem of three bodies. Technical report, Yale univ New Haven CT, 1967.
- [4] KC Howell and Henry J Pernicka. Numerical determination of lissajous trajectories in the restricted three-body problem. *Celestial Mechanics*, 41(1-4):107–124, 1987.
- [5] Aurélie Héritier and Kathleen C Howell. Natural regions near the collinear libration points ideal for space observations with large formations. *The Journal of the Astronautical Sciences*, 60(1):87–108, 2013.
- [6] M Hechler and A Yánez. Herschel/planck consolidated report on mission analysis. *MAO CReMA*, 3, 2001.
- [7] Henry J Pernicka, Brian A Carlson, and SN Balakrishnan. Spacecraft formation flight about libration points using impulsive maneuvering. *Journal of guidance, control, and dynamics*, 29(5):1122–1130, 2006.
- [8] Christopher GR Wallis, Michael L Brown, Richard A Battye, and Jacques Delabrouille. Optimal scan strategies for future cmb satellite experiments. *Monthly Notices of the Royal Astronomical Society*, 466(1):425–442, 2016.
- [9] Roberto Vieira da Fonseca Lopes Ronan Arraes Jardim Chagas. Seasonal analysis of attitude estimation accuracy for the brazilian satellite amazonia-1 under normal and faulty conditions. In *24th International Symposium on Space Flight Dynamics*. Instituto Nacional de Pesquisas Espaciais, 2014.
- [10] Radhika Radhakrishnan, William W Edmonson, Fatemeh Afghah, Ramon Martinez Rodriguez-Osorio, Frank Pinto, and Scott C Burleigh. Survey of inter-satellite communication for small satellite systems: Physical layer to network layer view. *IEEE Communications Surveys & Tutorials*, 18(4):2442–2473, 2016.
- [11] David Scharfe and Andrew Ketsdever. A review of high thrust, high delta-v options for microsatellite missions. In *45th AIAA/ASME/SAE/ASEE Joint Propulsion Conference & Exhibit*, page 4824, 2009.
- [12] Robert Osiander, M Ann Garrison Darrin, and John L Champion. *MEMS and microstructures in aerospace applications*. CRC press, 2018.